

## Task Space Division and Trajectory Planning for a Flexible Macro-Micro Manipulator System\*

LUO Lingzhi (罗凌智), ZHANG Yu (张宇), SUN Zengqi (孙增圻)\*\*

Department of Computer Science and Technology, Tsinghua University, Beijing 100084, China

**Abstract:** This paper deals with a flexible macro-micro manipulator system, which includes a long flexible manipulator and a relatively short rigid manipulator attached to the tip of the macro manipulator. A flexible macro manipulator possesses the advantages of wide operating range, high speed, and low energy consumption, but the disadvantage of a low tracking precision. The macro-micro manipulator system improves tracking performance by compensating for the endpoint tracking error while maintaining the advantages of the flexible macro manipulator. A trajectory planning scheme was built utilizing the task space division method. The division point is chosen to optimize the error compensation and energy consumption for the whole system. Then movements of the macro-micro manipulator can be determined using separate inverse kinematic models. Simulation results for a planar 4-DOF macro-micro manipulator system are presented to show the effectiveness of the control system.

**Key words:** macro-micro manipulator; trajectory planning; trajectory tracking control; task space division; flexible manipulator

### Introduction

With the development of space exploitation and exploration, a need has developed for mature robot manipulation technology for space missions. Flexible manipulators have played crucial roles in such applications for several decades due to their advantages such as large working range, high operating speed, and large payload to weight ratio. Several flexible manipulator systems have been put into use, such as the Canadian mobile servicing system (MSS)<sup>[1]</sup> mounted on the International Space Station. However, deformation and vibration of flexible links during high speed motion modeled with complex dynamics models result in large endpoint motion errors that can only complicate the

controller design.

The dynamic modeling and controller design of flexible manipulators have been studied by many researchers. For rigid-link manipulators, the dynamic equations can be derived using conventional methods such as Newton-Euler or Lagrangian formulations<sup>[2]</sup>. For the distributed flexible link, Cannon and Schmitz<sup>[3]</sup> and Hastings and Book<sup>[4]</sup> used the assumed modes method to model the flexible manipulator while Bayo<sup>[5]</sup> used Hamilton's principle and a finite element approach to model a single flexible-link manipulator. A closed-form finite-dimensional dynamic model for planar multilink lightweight robots was derived using the Lagrangian approach combined with the assumed modes method<sup>[6]</sup>. The use of rigid-link manipulator control methods for flexible manipulator results in greatly reduced tip positioning and tracking precision due to the structural flexibility and vibration of the flexible-link manipulator. Hashtrudi-Zaad and Khorasani<sup>[7]</sup> adopted an integral manifold method

---

Received: 2006-04-04; revised: 2006-12-18

\* Supported by the National Natural Science Foundation of China (No. 60305008)

\*\* To whom correspondence should be addressed.

E-mail: szq-dcs@mail.tsinghua.edu.cn; Tel: 86-10-62788939

which can be regarded as a form of output re-definition. In their paper, outputs were decomposed to fast and slow parts with the tracking problem then solved by tracking the slow output and stabilizing the fast one. Input-shaping control<sup>[8]</sup> has been used to effectively suppress tip vibrations through the convolution of a sequence of impulses with the reference input. However, such control methods, which are essentially open-loop control methods, are less robust and their performance depends greatly on the modeling precision. The singular perturbation theory<sup>[9]</sup> has also been introduced to model the two-time-scale nature of the system dynamics. The control strategy is then based on stabilizing the fast dynamics and tracking the joint trajectories. Yang et al.<sup>[10]</sup> proposed a compensation control method to reduce the tip errors by modulating the flexible manipulator actuators. However, the effectiveness of this control strategy is limited by the actual bandwidth of the joint actuators since the actuators must drive the motion of the flexible links at a lower frequency while adjusting the inputs to suppress vibration or compensate for tip errors at a higher frequency. The concept of a combined macro-micro architecture has been used to deal with these problems since the 1980s.

The flexible macro-micro manipulator combines a long, light flexible macro manipulator and a relatively short, rigid micro manipulator. Hogan et al.<sup>[11]</sup> examined the root locus and Bode plot of the force control to show that a macro-micro manipulator is inherently more stable in regulating interface forces than a conventional robot system. They developed a robust controller design based on physical equivalence and impedance matching. Interface force regulation at higher bandwidths could be achieved with only minimal knowledge of the structure. Sharf<sup>[12]</sup> used the reaction force from the micro manipulator to the macro manipulator as a control variable for damping the large flexible manipulator with simulation results for a 6-DOF rigid manipulator on a flexible mast demonstrating the feasibility of the approach. Yoshikawa et al.<sup>[13]</sup> used the concept of compensability of a flexible macro-micro manipulator to generate the joint trajectories and proposed a quasi-static trajectory tracking controller to track a circle as the desired tip trajectory. However, the tracking errors significantly increase as the system acceleration increases. A dynamic trajectory

tracking controller which analyzed the system dynamics was proposed to overcome the problem<sup>[14]</sup>. Motoyuki and Yoshifumi<sup>[15]</sup> presented a Lyapunov-based positioning controller for a 2-DOF macro-micro manipulator to suppress bending vibrations of the macro arm. A fuzzy controller<sup>[16]</sup> and a neural network controller<sup>[17]</sup> were introduced to improve motion control of the macro-micro manipulator.

This paper presents a new trajectory planning scheme to generate the joint trajectories which ensures that the planned tip position locates exactly on the desired point to improve the endpoint tracking accuracy. The endpoint tracking errors can be compensated by the additional motion of the micro manipulator. The controller adjusts the micro manipulator motion to compensate for the macro manipulator tip positioning errors due to deformation of the flexible links. Then the task space division approach is used to increase the feasibility of compensation by the micro manipulator and reduce the system energy consumption. The division point is determined by a genetic algorithm to guarantee optimization of the planned trajectories. Simulation results on a 4-DOF macro-micro manipulator demonstrate the effectiveness of the proposed methods.

## 1 Error Compensation Using Kinematics

### 1.1 Tip position error caused by deformation of the macro manipulator

Consider a robot system with an  $M$ -DOF macro manipulator and an  $m$ -DOF micro manipulator. Let  $\theta_M \in \mathbf{R}^M$  and  $\theta_m \in \mathbf{R}^m$  be the vectors of the joint variables of the macro-micro manipulator,  $\delta \in \mathbf{R}^e$  be the flexural displacement vector, and  $p \in \mathbf{R}^n$  be the tip vector in the  $n$ -dimensional task space. The end-point vector  $p$  is a nonlinear function of  $\theta_M$ ,  $\theta_m$ , and  $\delta$ :

$$p = f(\theta_M, \theta_m, \delta) \quad (1)$$

and the small displacements  $\tilde{p}$  of the tip vector can be expressed as

$$\tilde{p} = J_{\theta_M} \tilde{\theta}_M + J_{\theta_m} \tilde{\theta}_m + J_{\delta} \tilde{\delta} \quad (2)$$

where  $J_{\theta_M} \in \mathbf{R}^{n \times M}$ ,  $J_{\theta_m} \in \mathbf{R}^{n \times m}$ , and  $J_{\delta} \in \mathbf{R}^{n \times e}$  are Jacobian matrices of  $p$  with respect to  $\theta_M$ ,  $\theta_m$ , and  $\delta$ ; and  $\tilde{\theta}_M$ ,  $\tilde{\theta}_m$ , and  $\tilde{\delta}$  denote small changes in  $\theta_M$ ,  $\theta_m$ , and  $\delta$ .

The deflection of each flexible link can be approximated by a weighted summation of modes given by

$$\omega(x,t) = \sum_{i=1}^n \phi_i(x) \delta_i(t) \quad (3)$$

In this study, the first two dominant eigenmodes are taken into account to model the dynamic characteristics of the flexible macro manipulator. The deflection,  $\omega(x,t)$ , can be expressed in terms of the tip linear displacement,  $\varepsilon_i$ , and the tip angular deflection,  $\alpha_i$ , of flexible link  $i$ , which can be measured by an optical implement<sup>[10]</sup>.

The deflection of the flexible links can be converted to errors of the joint variables:

$$\tilde{\theta}_{\delta i} = \begin{cases} \varepsilon_i / l_i, & i = 1; \\ \alpha_{i-1} + \varepsilon_i / l_i, & 2 \leq i \leq M; \\ \alpha_M, & i = M + 1 \end{cases} \quad (4)$$

Equation (2) can then be rewritten to

$$\tilde{\mathbf{p}} = \mathbf{J}_{\theta_M} \tilde{\boldsymbol{\theta}}'_M + \mathbf{J}_{\theta_m} \tilde{\boldsymbol{\theta}}'_m \quad (5)$$

where

$$\tilde{\boldsymbol{\theta}}'_i = \begin{cases} \tilde{\theta}_i + \tilde{\theta}_{\delta i}, & 1 \leq i \leq M + 1; \\ \tilde{\theta}_i, & M + 2 \leq i \leq M + m \end{cases} \quad (6)$$

## 1.2 Micro manipulator motion adjustment

For a rigid link manipulator system, the end-point vector is a nonlinear function of  $\boldsymbol{\theta}_M$  and  $\boldsymbol{\theta}_m$

$$\mathbf{p} = \mathbf{f}(\boldsymbol{\theta}_M, \boldsymbol{\theta}_m, \mathbf{0}) \quad (7)$$

Compared to the physical parameters of the manipulators, tip errors caused by the deformation of the flexible links are small. To compensate such errors, the micro manipulator joint variables are adjusted as

$$\mathbf{f}(\boldsymbol{\theta}_M, \boldsymbol{\theta}'_m, \mathbf{0}) = \mathbf{f}(\boldsymbol{\theta}_M, \boldsymbol{\theta}_m, \mathbf{0}) + \tilde{\mathbf{p}} \quad (8)$$

where  $\boldsymbol{\theta}'_m$  denotes the joint variables after adjustment and  $\tilde{\mathbf{p}}$  can be updated by

$$\tilde{\theta}_i = 0, \quad 1 \leq i \leq M + m \quad (9)$$

Since the adjustments of  $\boldsymbol{\theta}_m$  are small, the resulting position change can be written as

$$\Delta \mathbf{f} = \mathbf{f}(\boldsymbol{\theta}_M, \boldsymbol{\theta}'_m, \mathbf{0}) - \mathbf{f}(\boldsymbol{\theta}_M, \boldsymbol{\theta}_m, \mathbf{0}) = \mathbf{J}_{\theta_m} (\boldsymbol{\theta}'_m - \boldsymbol{\theta}_m) \quad (10)$$

Equations (5), (6), (8)-(10) can be combined as

$$\begin{aligned} \boldsymbol{\theta}'_m &= \boldsymbol{\theta}_m + \mathbf{J}_{\theta_m}^+ (\mathbf{J}_{\theta_M} \tilde{\boldsymbol{\theta}}'_M + \mathbf{J}_{\theta_m} \tilde{\boldsymbol{\theta}}'_m) = \\ &(\boldsymbol{\theta}_m + \tilde{\boldsymbol{\theta}}'_{\delta m}) + \mathbf{J}_{\theta_m}^+ \mathbf{J}_{\theta_M} \tilde{\boldsymbol{\theta}}'_M \end{aligned} \quad (11)$$

where  $\mathbf{J}_{\theta_m}^+$  denotes the pseudo-inverse matrix of  $\mathbf{J}_{\theta_m}$ ,  $\tilde{\boldsymbol{\theta}}'_{\delta M} \in \mathbf{R}^M$  and  $\tilde{\boldsymbol{\theta}}'_{\delta m} \in \mathbf{R}^m$  denote the equivalent joint

variables changes of the macro and micro manipulators due to the deformation of the flexible links of the macro manipulator:

$$\tilde{\boldsymbol{\theta}}'_{\delta M} = [\tilde{\theta}_{\delta 1}, \tilde{\theta}_{\delta 2}, \dots, \tilde{\theta}_{\delta M}]^T \quad (12)$$

$$\tilde{\boldsymbol{\theta}}'_{\delta m} = [\tilde{\theta}_{\delta(M+1)}, 0, \dots, 0]^T \quad (13)$$

## 2 Trajectory Planning by Task Space Division

For a macro-micro manipulator, in general, the number of actuators is more than that of the task space dimension. That is, the macro-micro manipulator is a redundant system for trajectory tracking. Therefore, the system will have an infinite number of solutions for the joint variables that can make the tip position exactly follow the desired trajectory. Among all these possible solutions, some of the solutions are expected to facilitate compensation and improve the tracking. A differential method was chosen to improve the compensation<sup>[13]</sup>. However, the parameter selection is not guided by specific criteria so an optimal solution cannot be guaranteed.

Since the objective of this analysis is to only consider the trajectory tracking problem, the analysis will consider only a special redundant macro-micro manipulator with the same number of actuators as the task space dimension. Therefore, the separately macro and micro manipulators are not redundant, but the system as a whole is redundant.

### 2.1 Task space division utilizing redundancy

The task space is divided into two parts for the macro manipulator and the micro manipulator. The macro manipulator carries the micro manipulator to the neighborhood of the task point, and then the micro manipulator sets its joint variables to put the tip on the task point.

$$\mathbf{p} = \mathbf{p}_M + \mathbf{p}_m \quad (14)$$

where  $\mathbf{p}_M$  denotes the vector of the task division point, which is the end-point of the macro manipulator and the base point of the micro manipulator;  $\mathbf{p}_m$  denotes the vector from the division point to the tip of the micro manipulator.

In this task division scheme, the joint variables are determined with the task division point because the number of actuators for the macro-micro manipulator

is equal to the task space dimension.

$$\mathbf{p}_M = \mathbf{f}_M(\boldsymbol{\theta}_M) \quad (15)$$

$$\mathbf{p}_m = \mathbf{f}_m(\boldsymbol{\theta}_m) \quad (16)$$

With the task division, the joint variables,  $\boldsymbol{\theta}_M$  and  $\boldsymbol{\theta}_m$ , can be directly determined by the inverse kinematics with the shape selected to facilitate the compensation:

$$\boldsymbol{\theta}_M = \mathbf{f}_M^{-1}(\mathbf{p}_M) \quad (17)$$

$$\boldsymbol{\theta}_m = \mathbf{f}_m^{-1}(\mathbf{p}_m) \quad (18)$$

The planned tip position is required to be exactly the task point in Eq. (14). In addition to Eq. (14), two inequalities must also be satisfied to guarantee the existence of solutions for Eqs. (17) and (18):

$$\|\mathbf{p}_M\| \leq \sum_{i=1}^M l_i \quad (19)$$

$$\|\mathbf{p}_m\| \leq \sum_{i=M}^{M+m} l_i \quad (20)$$

where  $\|\cdot\|$  denotes the Euclidean norm of the vector.

Considering the mechanical limitations of the micro manipulator, the division point must be in a circle with the task point as its center and  $\sum_{i=1}^m l_{M+i}$  as its radius.

## 2.2 Division point selection algorithm

Any given tip position has an infinite number of solutions for the joint variables due to the system redundancy. Therefore, an optimal solution can be selected to simplify the compensation and reduce the energy consumption in the tracking. After the task space division, the number of solutions equals the number of division points in the circle of Eq. (20).

A genetic algorithm was used to select the optimal division point which satisfied the two criteria in Eqs. (19) and (20).

$$\text{Define } \Delta\boldsymbol{\theta}_m = \boldsymbol{\theta}'_m - \boldsymbol{\theta}_m \quad (21)$$

According to Eq. (11)

$$\Delta\boldsymbol{\theta}_m = \tilde{\boldsymbol{\theta}}'_{\delta_m} + \mathbf{J}_{\theta_m} + \mathbf{J}_{\theta_M} \tilde{\boldsymbol{\theta}}'_{\delta_M} \quad (22)$$

From Eqs. (4) and (12)

$$\tilde{\boldsymbol{\theta}}'_{\delta_m} = \mathbf{T}_\varepsilon \boldsymbol{\varepsilon} + \mathbf{T}_\alpha \boldsymbol{\alpha} \quad (23)$$

where  $\boldsymbol{\varepsilon} = [\varepsilon_1, \dots, \varepsilon_M]^\top$ ,  $\boldsymbol{\alpha} = [\alpha_1, \dots, \alpha_M]^\top$ , and  $\mathbf{T}_\varepsilon$  and  $\mathbf{T}_\alpha$  are given as

$$\mathbf{T}_\varepsilon = \frac{\partial \tilde{\boldsymbol{\theta}}'_{\delta_M}}{\partial \boldsymbol{\varepsilon}} = \text{diag}[l_1, l_2, \dots, l_M]^{-1} \quad (24)$$

$$\mathbf{T}_\alpha = \frac{\partial \tilde{\boldsymbol{\theta}}'_{\delta_M}}{\partial \boldsymbol{\alpha}} = \begin{bmatrix} 0 & 0 & \cdots & 0 \\ 1 & 0 & \ddots & \vdots \\ 0 & \ddots & \ddots & 0 \\ 0 & 0 & 1 & 0 \end{bmatrix} \quad (25)$$

Let  $\text{diag}[\cdot]$  denote the diagonal matrix.

Substitute Eq. (23) into Eq. (22)

$$\Delta\boldsymbol{\theta}_m = \mathbf{J}_\varepsilon \boldsymbol{\varepsilon} + \mathbf{J}_\alpha \boldsymbol{\alpha} = \mathbf{J}_\delta \tilde{\boldsymbol{\delta}} \quad (26)$$

where  $\mathbf{J}_\delta = [\mathbf{J}_\varepsilon \quad \mathbf{J}_\alpha]$ ,  $\mathbf{J}_\varepsilon = \mathbf{J}_{\theta_m} + \mathbf{J}_{\theta_M} \mathbf{T}_\varepsilon$ ,  $\mathbf{J}_\alpha = \mathbf{J}_{\theta_m} + \mathbf{J}_{\theta_M} \mathbf{T}_\alpha + [1 \quad 0 \quad \dots \quad 0]^\top$ , and  $\tilde{\boldsymbol{\delta}} = [\boldsymbol{\varepsilon} \quad \boldsymbol{\alpha}]^\top$ .

The deformation  $\tilde{\boldsymbol{\delta}}$  is normalized based on the weight of each element

$$\tilde{\boldsymbol{\delta}}_{\text{norm}} = \mathbf{T}_\delta \tilde{\boldsymbol{\delta}} \quad (27)$$

where

$$\mathbf{T}_\delta = \text{diag}[\varepsilon_{1,\max}, \dots, \varepsilon_{M,\max}, \alpha_{1,\max}, \dots, \alpha_{M,\max}]^{-1} \quad (28)$$

Here,  $\varepsilon_{i,\max}$  and  $\alpha_{i,\max}$  ( $i=1, 2, \dots, M$ ) denote the weights of each element of  $\tilde{\boldsymbol{\delta}}$ . The micro manipulator joint displacement,  $\Delta\boldsymbol{\theta}_m$ , for compensation are also normalized to take the cost of each micro manipulator joint into consideration:

$$\Delta\tilde{\boldsymbol{\theta}}_m = \mathbf{T}_m \Delta\boldsymbol{\theta}_m \quad (29)$$

where

$$\mathbf{T}_m = \text{diag}[\theta_{m1,\text{cost}}, \theta_{m2,\text{cost}}, \dots, \theta_{mm,\text{cost}}]^{-1} \quad (30)$$

Here,  $\theta_{mi,\text{cost}}$  ( $i=1, 2, \dots, m$ ) denotes the cost of each micro manipulator joint.

From Eq. (26)

$$\Delta\tilde{\boldsymbol{\theta}}_m = \tilde{\mathbf{J}}_\delta \tilde{\boldsymbol{\delta}}_{\text{norm}} \quad (31)$$

where  $\tilde{\mathbf{J}}_\delta = \mathbf{T}_m \mathbf{J}_\delta \mathbf{T}_\delta^{-1}$ . To minimize  $\|\Delta\tilde{\boldsymbol{\theta}}_m\|$  for any  $\tilde{\boldsymbol{\delta}}_{\text{norm}}$  satisfying  $\|\tilde{\boldsymbol{\delta}}_{\text{norm}}\| \leq 1$ , the compensability is measured by

$$I_c = \frac{1}{\|\tilde{\mathbf{J}}_\delta \tilde{\mathbf{J}}_\delta^\top\|} \quad (32)$$

which should be as small as possible as the first optimization objective.

Another objective is the joint angle change from one state to another state, which represents the energy consumption

$$I_e = \lambda \left[ \sum_{i=1}^M k_{Mi} (\theta_{Mi} - \theta_{Mi0})^2 + \sum_{i=1}^m k_{mi} (\theta_{mi} - \theta_{mi0})^2 \right] \quad (33)$$

where the constant  $\lambda$  is chosen so as to make  $I_c$  and  $I_e$  comparable.

The optimization function is then

$$G(\theta_M, \theta_m) = a_1 I_c + a_2 I_e \quad (34)$$

where  $a_1$  and  $a_2$  denote the weights of  $I_c$  and  $I_e$  in the optimization function.

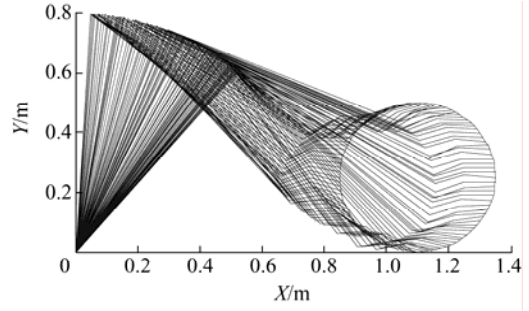
In the genetic algorithm, the circle space of the division points is discretized into elements that are encoded by their coordinates in a 0-1 series. Due to the circular shape of the space, initialization, crossover, and mutation operations must avoid generating codes which represent points outside the boundary of the circle. The optimization function in Eq. (34) is evaluated for each generated legal division point as the fitness values.

### 3 Simulation Results

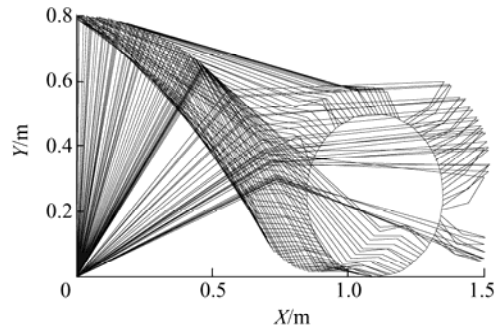
The effectiveness of the trajectory planning scheme was evaluated for a planar 4-DOF macro-micro manipulator. The flexible macro manipulator and the rigid micro manipulator are both 2-DOF systems. The geometric parameters of the macro-micro manipulator are as follows.  $l_1, l_2$  are 0.5 m and  $l_3, l_4$  are 0.16 m.

The desired circular tip trajectory is prescribed starting from the initial point (1.1, 0) with (1.1, 0.5) as its center. The desired reference joint trajectories are generated by the inverse dynamics. The initial system state is obtained by the genetic algorithm with  $a_1=1$  and  $a_2=0$  in Eq. (34). A second state is determined with  $a_1=1$  and  $a_2=1$ . Here,  $\lambda$  is 2.5. The final planned joint trajectory considering both the compensation ability and the energy consumption is shown in Fig. 1a. The trajectories for the case in Fig. 1b where  $a_1=1$  and  $a_2=0$  do not include the consideration of the energy consumption, while the trajectories for the case in Fig. 1c where  $a_1=0$  and  $a_2=1$  do not include the consideration of the compensability.

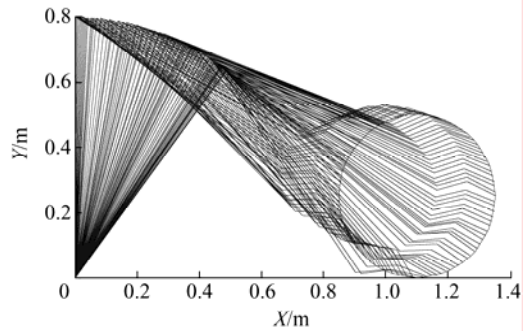
The angles of the four joints are shown in Fig. 2 for these three cases with the compensability for each case. The joint angles change more rapidly if the energy consumption is less important in the optimization function of Eq. (34) with the compensability for the case in Fig. 2b larger than for the cases in Figs. 2a and 2c. Generally, the compensability increases with the weight  $a_1$  in Eq. (34); however, there are some positions in Fig. 3 where the compensability for the case B is less due to the initial states.



(a) Considering compensability and energy consumption ( $a_1=1$  and  $a_2=1$ )



(b) Considering only compensability ( $a_1=1$  and  $a_2=0$ )

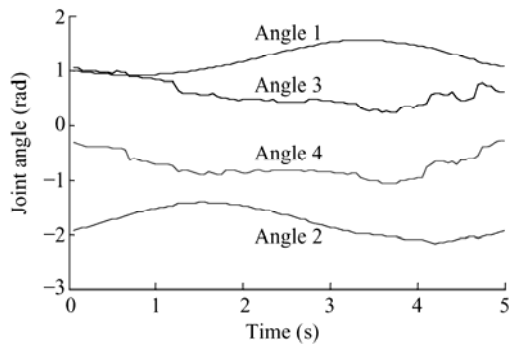


(c) Considering only energy consumption ( $a_1=0$  and  $a_2=1$ )

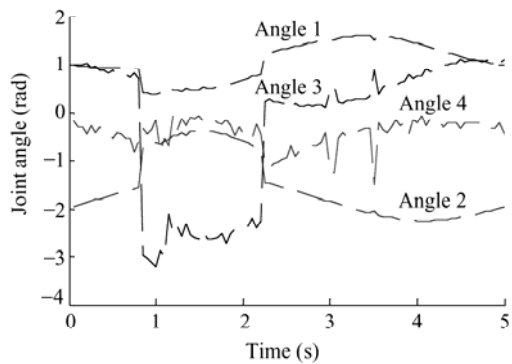
**Fig. 1 Planned joint trajectories**

Figure 4 shows how the fitness changes from generation to generation in the genetic algorithm. The optimal fitness can be selected from the 100 generations. The compensation effectiveness of compensability was tested by adding a sine wave disturbance with amplitude 0.05 as the deformation  $\tilde{\delta}$ .

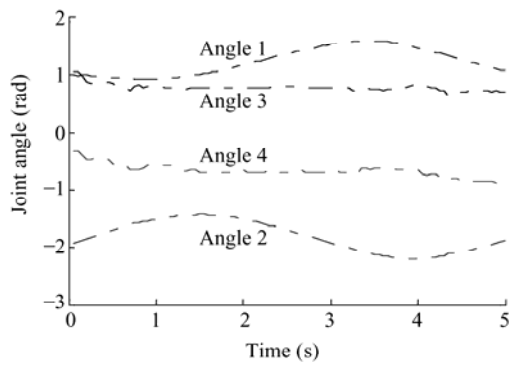
The adjustments of the micro manipulator joint angles are shown in Fig. 5. Figure 5a is for a fixed micro manipulator representing a flexible manipulator without macro-micro architecture. Figure 5b has the division point set on the desired tip position so the micro manipulator does not take part in the trajectory planning but functions only to compensate for the deformation errors. Figure 5c has the micro manipulator as part



(a) Considering compensability and energy consumption ( $a_1=1$  and  $a_2=1$ )



(b) Considering only compensability ( $a_1=1$  and  $a_2=0$ )



(c) Considering only energy consumption ( $a_1=0$  and  $a_2=1$ )

**Fig. 2 Planned joint angles**

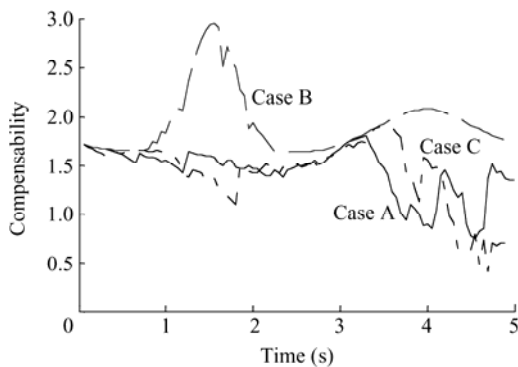


**Fig. 3 Compensability for the three cases**

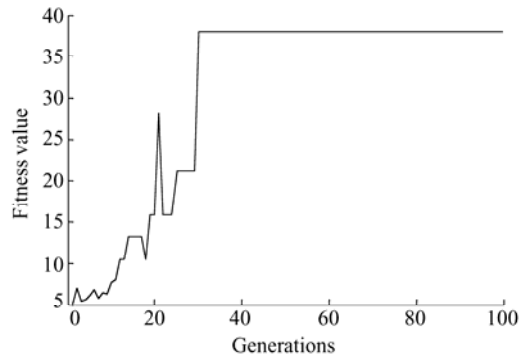
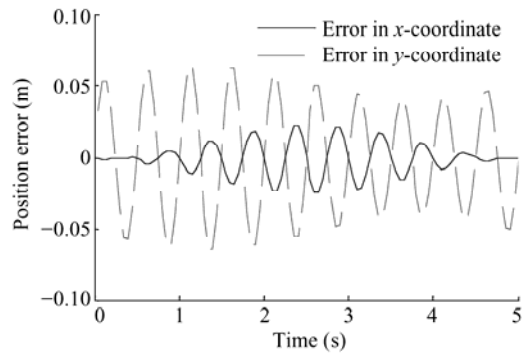
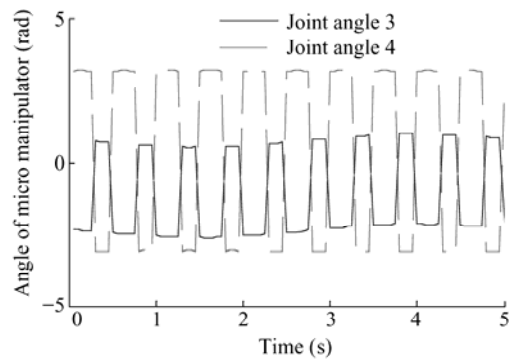


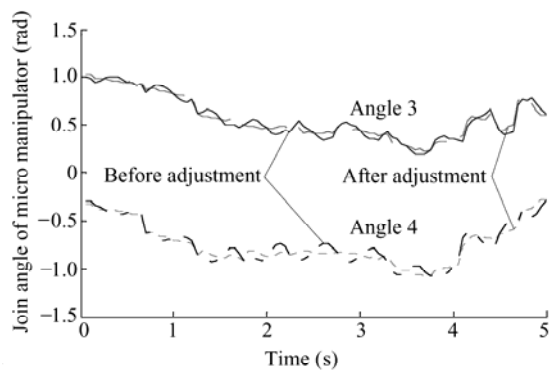
**Fig. 4 Fitness changes during the genetic algorithm calculations**



(a) Fixed micro manipulator



(b) Joint angle without micro manipulator for planning



(c) Joint angle before and after adjustments

**Fig. 5 Tip positions and joint angles with a sinusoid disturbance**

of the trajectory planning and the deformation compensation. The results in Fig. 5a show that large tip position errors caused by deformations of the flexible links cannot be easily compensated for due to the bandwidth limitations of the actuators. The system in Fig. 5b leads to frequent and rapid changes of the micro manipulator joint angles. The complete system in Fig. 5c results in smooth curves for the joint angles with small changes to compensate for the disturbance which demonstrates the effectiveness of the trajectory planning scheme.

## 4 Conclusions

A kinematic compensation method is given to alleviate tip positioning errors in a flexible macro-micro manipulator caused by deformations and vibrations in the linkages. The algorithm is based on a trajectory generation method which uses task space division and the selection of optimal division points. The optimization function includes the compensability and the energy consumption. A genetic algorithm is used to search for the optimal points in a circle. Simulation results for a 2-DOF macro/ 2-DOF micro manipulator show the effectiveness of the proposed methods.

## References

- [1] Sallaberger C. Robotics and control R & D in the Canadian space station program. In: Proc. of Canadian Conference on Electrical and Computer Engineering. Calgary, Canada, 1996: 482-485.
- [2] Spong M, Vidyasagar M. Robot Dynamics and Control. New York: Wiley and Sons, 1989.
- [3] Cannon R H, Schmitz E. Initial experiments on the end-point control of a flexible one-link robot. *International Journal of Robotics Research*, 1984, **3**(3): 62-75.
- [4] Hastings G, Book W J. Experiments in the optimal control of a flexible link manipulator. In: American Control Conference. Boston, USA, 1985: 728-729.
- [5] Bayo E. A finite-element approach to control the end-point motion of a single-link flexible robot. *Journal of Robotic Systems*, 1987, **4**(1): 63-75.
- [6] Luca A D, Siciliano B. Closed-form dynamic model of planar multilink lightweight robots. *IEEE Transactions on Systems, Man, and Cybernetics*, 1991, **21**(4): 826-839.
- [7] Hashtrudi-Zaad K, Khorasani K. Control of nonminimum phase singularly perturbed systems with applications to flexible link manipulators. *International Journal of Control*, 1996, **63**(4): 679-701.
- [8] Tzes A, Yurkovich S. An adaptive input shaping control scheme for vibration suppression in slewing flexible structures. *IEEE Transactions on Control Systems Technology*, 1993, **1**(2): 114-121.
- [9] Lewis F L, Vandegrift M. Flexible robot arm control by a feedback linearization singular perturbation approach. In: Proceedings of IEEE International Conference on Robotics and Automation. Atlanta, USA, 1993: 729-736.
- [10] Yang T W, Xu W L, Tso S K. Dynamic modeling based on real-time deflection measurement and compensation control for flexible multi-link manipulators. *Dynamics and Control*, 2001, **11**: 5-24.
- [11] Hogan N, Sharon A, Hardt E D. High bandwidth force regulation and inertia reduction using a macro/micro manipulator system. In: Proc. of IEEE Conference on Robotics and Automation. Phila., PA, USA, 1988: 126-132.
- [12] Sharf I. Active damping of a large flexible manipulator with a short-reach robot. *ASME Journal of Dynamic Systems Measurement and Control*, 1996, **118**: 704-713.
- [13] Yoshikawa T, Hosoda K, Doi T, Murakami H. Quasi-static trajectory tracking control of flexible manipulator by macro-micro manipulator system. In: Proceedings of IEEE International Conference on Robotics and Automation. Atlanta, USA, 1993: 210-215.
- [14] Yoshikawa T, Hosoda K, Doi T, Murakami H. Dynamic trajectory tracking control of flexible manipulator by macro-micro manipulator system. In: Proceedings of IEEE International Conference on Robotics and Automation. San Diego, USA, 1994: 1804-1809.
- [15] Motoyuki K, Yoshifumi M. PDS control of macro-micro arm. In: Proceedings of the 8th IEEE International Workshop on Advanced Motion Control. Kawasaki, Japan, 2004: 123-128.
- [16] Mannami A, Talebi H A. A fuzzy Lyapunov-based control strategy for a macro-micro manipulator. In: Proceedings of IEEE Conference on Control Applications. Istanbul, Turkey, 2003: 368-373.
- [17] Cheng X P, Patel R V. Neural network based tracking control of a flexible macro-micro manipulator system. *Neural Networks*, 2003, **16**: 271-286.